

## Material Science and Engineering with Advanced Research

### On the Cold Rolling of Explosive Welded Al/Cu Bimetallic Sheets

AK Polyzou<sup>1</sup>, GV Seretis<sup>1</sup>, N Vaxevanidis<sup>2</sup>, CG Provatidis<sup>1</sup> and DE Manolakos<sup>1</sup>

<sup>1</sup>National Technical University of Athens, School of Mechanical Engineering, HeroonPolytechniou 9, 15780 Zografou, Athens, Greece

<sup>2</sup>School of Pedagogical and Technological Education, Department of Mechanical Engineering Educators, 14121 N. Heraklion, Athens, Greece

**\*Corresponding author:** N. Vaxevanidis, School of Pedagogical and Technological Education, Department of Mechanical Engineering Educators, 14121 N. Heraklion, Athens, Greece; E mail: vaxev@aspete.gr

**Article Type:** Research, **Submission Date:** 03 February 2017, **Accepted Date:** 15 March 2017, **Published Date:** 06 June 2017.

**Citation:** AK Polyzou, GV Seretis, N Vaxevanidis, CG Provatidis and DE Manolakos (2017) On the Cold Rolling of Explosive Welded Al/Cu Bimetallic Sheets. Mater. Sci. Eng. Adv. Res Special Issue: 34-44. doi: <https://doi.org/10.24218/msear.2017.55>.

**Copyright:** © 2017 AK Polyzou, et al. This is an open-access article distributed under the terms of the Creative Commons Attribution License, which permits unrestricted use, distribution, and reproduction in any medium, provided the original author and source are credited.

#### Abstract

The explosive welding method has a wide range of applications, which is still growing. A rapid worldwide growth of interest is evident, since the use of multi-layer materials is becoming increasingly vital for the industry. However, the materials produced by explosive welding rarely possesses their final application characteristics. Therefore, post-welding processes are in most of the cases necessary to form or improve the properties of the product of explosive welding. This paper describes a study on the suitability of cold rolling processes for formation and/or properties' improvement of explosively welded bimetallic aluminum-copper specimens. Two different cold rolling processes are tested. The rolling process products are examined as regards their hardness and the microstructure of the intermetallic layer on the bonding surface. Defects, such as lateral spread, observed during cold rolling are also evaluated.

**Keywords:** Rolling, Explosive welding, Aluminum, Copper, Bimetallic strip.

#### Introduction

In last decades, a growing need for metallic materials of special requirements regarding their properties has been risen. In many cases, these materials should response by activating two or more different deformation mechanisms under loading and consequently their properties should vary along their thickness. Therefore, a great part of the research interest on this field focused on multilayer metallic materials, which are able to meet the new demanding specifications by bonding metals with dissimilar properties. However, a strong bond in very dissimilar metals welding is often impractical to be achieved by conventional fusion welding. As a solution for this problem, the explosive welding process can be applied. Explosive welding or cladding is a solid-state technique in which the detonation of a

certain amount of an explosive is used to accelerate one of the materials in order to promote a high velocity oblique collision. This collision produces pressures high enough to cause excessive plastic deformation at the interface and mixing of the surface layers of materials to be bonded which can result in a linear or a wavy interface in explosively welded joints.

A considerable number of studies have dealt with the configuration of the explosive welding process and the simulation of the explosive welding mechanism [1-14]. Lysak & Kuzmin [1] used a calorimetric method to determine the portion of the energy transferred to the flyer plate and reached the conclusion that this amount of energy does not exceed 1% of the total energy of the explosion. In the same study it was also shown that during the collision of explosively welded plates, a portion of the kinetic energy of the flyer plate transforms into other types of energy and is also released as heat. Mendes et al. [2] examined the influence of explosive characteristics on the weld interfaces of stainless steel AISI 304L to low alloy steel 51CrV4 in a cylindrical configuration and showed that the type of explosive and the type and proportion of explosive sensitizers affect the main welding parameters, particularly collision point velocity. The effect of explosive welding parameters on metallurgical and mechanical interfacial features of Inconel 625/plain carbon steel bimetal plate was examined by Rajani & Mousavi [3] who related the load ratio and standoff distance as two main explosive welding parameters to interfacial features of explosive clad Inconel 625/plain carbon steel bimetal plate such as interfacial structure, interfacial local melting phenomenon, localization of plastic strain, hardness variation across the interface and adhesion strength. Wang et al. [4] introduced the usage of the material point method (MPM) in numerical simulation of explosive welding, attaining important technical parameters for the explosive welding on the MPM simulation. Smoothed Particle Hydrodynamics (SPH) method

was used by Xiao Wang et al. [5] on a numerical study of the mechanism of the explosive/impact welding, who showed in this study that although it is found that bonding is more likely to be a solid state welding process, however, in some cases, it is likely to be a fusion welding process. A series of numerical and experimental studies of the mechanism of the wavy interface formations in explosive/impact welding performed by Mousavi et al. [6], using a finite difference engineering package to model the oblique impact of a thin flyer plate on a relatively thick base. Athar & Tolaminejad [7] calculated the weldability criteria which should be met in order to achieve a good welding quality for Al/Cu/Al explosively welded bimetallic sandwich. Akbari Mousavi et al. [8] also simulated the welding process using a finite element-based computer model. Wypart et al. [9] investigated the effect of plastic deformation and heat treatment on the properties of joint area of AL99,8 + M1E bimetallic plate. In this study, the joining zones were analyzed after rolling in three variants: directly after joining, after joining and annealing at 300°C, and after joining and annealing at 400°C. Experimental and computational analysis of aluminum to aluminum explosive welding was also performed by Grignon et al. [13]; this study concerned with the so-called "Mars Sample Return Mission".

Microstructure and intermetallic compounds which are developed during the explosive welding process on the welding surface have also been extensively studied [15-26]. The elastic and thermodynamic properties of Al-Cu intermetallic compounds have been investigated by using the first-principles density functional theory (DFT) within the generalized gradient approximation (GGA) by Chen et al. [15]. The fatigue behavior of Cu-Al interfaces, focusing on the role of the intermetallic compounds on this behavior, has been studied by Lassnig et al. [16]. Bataev et al. [17] examined the structural and mechanical properties of metallic-intermetallic laminate composites produced by explosive welding and annealing under tension tests and impact strength tests. This study focused on the effect of the annealing time on the intermetallic layer growth. Microstructural inhomogeneity and mechanical properties of explosive welded 2205 stainless steel/X65 steel bimetallic sheets were investigated by Zhang et al. [18] who reported that voids were prone to appear in the peninsula and island morphologies near the interface. Kahraman et al. [19] observed that grains near the interface were elongated parallel to the explosion direction in a study on joining of titanium/stainless steel by explosive welding, whilst the effect of annealing on the interface microstructure and on mechanical characteristics of AZ31B/AA6061 composite plates fabricated by explosive welding was examined by Zhang et al. [20]. In this study, they reported that on annealing at and above 250 °C, intermetallic compounds of Al<sub>3</sub>Mg<sub>2</sub> and Al<sub>12</sub>Mg<sub>17</sub> were observed to exist at the bonding interface. Xie et al. [21] examined the microstructure of CP-Ti/X65 bimetallic sheets fabricated by explosive welding before and after hot rolling. A metallographic examination of copper/

stainless steel joints formed by explosive welding was performed by Durgutlu et al. [22] who reported that diffusion did not take place between bonding plates, however, diffusion was observed after annealing of the bonded samples for different times. Song et al. [23] investigated the effect of Si additions on the intermetallic compound layer of 5A06 aluminum alloy and AISI 321 stainless steel. The different morphologies for welding interface obtained by changing the welding parameters were investigated by Athar & Tolaminejad [7]. The weldability criteria which should be met to achieve good welds for aluminum-copper joints were also reported; in addition, an effort for establishing a relation between microstructure and parameters of the process can be found in this study. The wave formation at the explosive welding interface was analytically studied by Cowan et al. [24] who investigated the mechanism of bond zone wave formation; Jaramillo et al. [25] who investigated the transition from a waveless to a wavy interface in exploding welding and Bazdenkov et al. [26] who proposed possible mechanism of wave formation in explosive welding.

Summarizing the research reported in [1-26] it should be noted that theories suggested for wave formation in explosive welding belong to the following categories: Indentation mechanism, flow instability mechanism, vortex shedding mechanism and stress wave mechanism [6,7,26]. Another mechanism was proposed based on the similarity between the interfacial waves in explosive welding and von Karman's vortex streets generated behind an obstacle [24].

Moreover, in many cases it has been reported that the final multi-layer product's properties of the explosive welding process needed improvement or further forming operations. Thus, a need for post-welding processes which would be able to deal with this challenge emerged [10]. Asemabadi et al. [27] investigated the influence of a cold rolling process on the mechanical properties and the bond strength of Al/Cu/Al sandwich specimen fabricated by explosive welding. In their study, the mechanical properties of the raw materials and the cold-rolled samples were experimentally determined using the tensile, tensile-shearing and hardness tests along the thicknesses of the samples, as well as fractography of the fracture surfaces after the tensile tests. An investigation of the structural and mechanical properties of metallic-intermetallic laminate composites produced by explosive welding after annealing under an air atmosphere of 630 °C with time variation from 1 to 100 hours was performed by Bataev et al. [17]. The effect of a hot rolling process on the mechanical properties of CP-Ti/X65 bimetallic sheets fabricated by explosive welding was examined by Xie et al. [21].

Using the explosive welding method, the desired thickness of the sheet is rarely obtained. Therefore, it is essential to apply the second post-welding process, which is, in a great variety of applications, the rolling process. However, when an intermetallic compound has been formed during the welding process (mostly in the form of a global or local layer), it is important

that the post-welding process does not affect the structure of this brittle layer. The aim of the present study is to investigate the formability, as regards cold rolling, of explosively welded bimetallic Al/Cu specimens and to determine if a cold rolling process is able to reduce their thickness and improve their properties without affecting the intermetallic layer, through hardness and metallographic investigation. To achieve this objective, two different cold rolling schemes were performed on the explosively welded specimens and the rolled specimens underwent Vickers hardness measurements and optical and scanning electron microscopic examination. A comparison of the results of the different rolling processes is provided together with the conclusions on the suitability of the cold rolling process for post-welding treatment of the Al/Cu explosively welded specimens.

## Experimental

### Material and specimens

Two explosively welded bimetallic aluminum-copper specimens, A and B, were used for the experiments, as shown in Figure 1. Specimens A and B, with dimensions 53.30 mm × 13.70 × 8.80 mm and 53.25 mm × 13.70 × 8.75 mm, respectively, underwent two different cold rolling pass sequences.



Figure 1: An explosively welded bimetallic specimen

For the explosive welding experiments, the following materials were used:

A copper plate (DHP-SU<sup>®</sup>) with phosphorus content 0.01 % was used as fixed (parent) plate. The dimensions of this plate were 210 mm × 60 mm × 4 mm.

An aluminum alloy of 5000 series plate with magnesium 1 % and

iron 0.75 %t was used as flyer plate. This plate's dimensions were 215 mm × 70 mm × 5 mm.

A steel lamina of high hardness was used as driving plate. This plate's dimensions were 200 mm × 60 mm × 2.9 mm.

### Experimental set-up and procedure

**Explosive welding:** The explosive welding set-up is presented schematically in Figure 2. The explosive material (detonator) used was ammonium nitrate of low defusing speed (ANFO), with granular oil content 6 % and packing density 0.85 g/cm<sup>3</sup>. In order to avoid the creation of an unstable defusing front, the booster explosive material PETN of 7000 m/s defusing speed was also used. The explosive welding arrangement was inclined with positioning angle  $\alpha=6^\circ$ . Table 1 shows the parameters of the explosive welding operation. The dimensions of the explosive welded specimens are presented in Table 2.

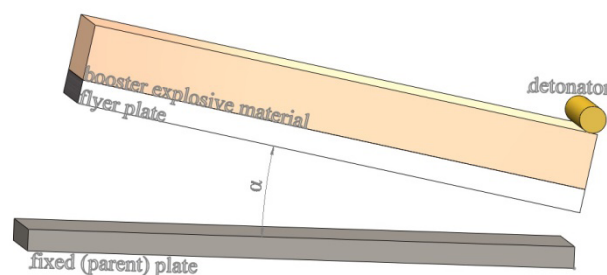


Figure 2: Experimental set-up of explosive welding

**Cold rolling:** The rolling mill used for the present series of experiments consisted of two hardened steel rolls of diameter  $D=200$  mm and width  $L=100$  mm. The body of the rolling mill was made of cast iron. The rollers were connected with an asynchronous gearmotor of 7 KW power and their rotational speed was varying from 3.3 to 20 rpm. Two KISTLER<sup>®</sup> converters of 40 tn maximum capacity, adjusted on the mounting of the upper roller, were used to monitor the load throughout the experiments. To monitor the torque, two KYOWA<sup>®</sup> torque

Table 1: Parameters of the explosive welding

Dimensions of flyer plate (Al)	215 mm × 70 mm × 5 mm
Dimensions of fixed plate (Cu)	210 mm × 60 mm × 4 mm
Dimensions of driving plate (St)	200 mm × 60 mm × 2.9 mm
Initial positioning angle ( $\alpha$ )	6°
Impact angle ( $\beta$ )	16.1°
Clearance	6 mm
Thickness of explosive material ( $h_e$ )	40 mm
Rate of explosive load (R)	1.05
Speed of accelerated plate ( $u_p$ )	359 m/s

Table 2: Dimensions of all explosively welded bimetallic specimens tested

Specimen	Total thickness [mm]	Al thickness [mm]	Cu thickness [mm]	Length [mm]	Al width [mm]	Cu width [mm]
A	8.80	4.20	4.60	53.30	13.70	13.70
B	8.75	4.15	4.60	53.25	13.60	13.80

converters were also used. Additionally, a KISTLER<sup>®</sup> 5011 power amplifier and a HBM<sup>®</sup> ME30 torque amplifier were used, both calibrated according to the manufacturer's instructions. The final curve recording was performed through the LAB VIEW<sup>®</sup> software.

Both specimens underwent a series of passes of cold rolling without lubrication. The decrease of the total thickness and the thickness of each layer of the bimetallic specimens, as well as the change of the width and the length of the two components of the specimens, were measured after each pass using an electronic digital caliper. Specimen A underwent 11 passes of cold rolling with 0.5 mm thickness reduction in each pass. Specimen B underwent 6 passes of cold rolling with 1 mm thickness reduction in each pass.

**Hardness measurements:** Before and after each experiment, Vickers hardness of each layer of the specimens was measured, using a WolpertDiaTestor 2rc hardness measuring machine. For these measurements the weight was 5 kp and the application time 15 s. To ensure the accuracy, three measurements were performed on each specimen.

**Metallographic observation:** In order to perform a metallographic study of the specimens, each one of them cut transversely and boxed using ACRYFIX resin. The cross section surface was mechanically ground using SiC paper (grid 220, 500, 800, 1200, 2400 and 4000). Subsequently, it was polished using velvet paper with diamond grains. During the polishing process, liquid alumina solution was added. The polished specimens washed with ethanol and dried. A LEICA DMR optical microscope was used for the metallographic study. Furthermore,

to investigate the intermetallic compounds resulted from the explosive welding process, before the cold rolling operation, a Philips XL 40SFEG scanning electron microscope (SEM) with an incorporated EDAX EDS analyzer was used for further investigation of the specimens.

## Results and discussion

All the parameters of the cold rolling for specimens A and B are presented in Table 3 and Table 4, respectively. Table 5 shows the variation of the dimensions of specimens A and B occurred from the cold rolling process. The average values of the Vickers hardness tests, before and after cold rolling, for both specimens can be found in Table 6. Figures 3-5 present the variation of the total rolling force, the total rolling torque and the lateral spreading in relation to total thickness reduction, respectively, for both specimens.

The microstructure of the Al/Cu interface of the explosively welded specimens A, as observed using the optical microscope, are presented in Figures 6-7, together with a series of photographs showing partially and more focused the whole interface, see Figure 7. Scanning electron micrographs and elemental microanalysis spectrum of the same specimen before cold rolling, as observed in a scanning electron microscope (SEM), are shown in Figure 8. The chemical composition of the intermetallic compound is presented in Table 7.

### Deformation behavior of the bimetallic specimens

The forming processes used for this study did not involve any heat treatment of the specimens, neither before rolling, nor at any stage between rolling passes. Due to the lack of heat treatments,

**Table 3:** Parameters of cold rolling for specimen A

Rolling pass number <i>i</i>	Total thickness <i>h<sub>T</sub></i> (mm)	Total thickness reduce <i>r<sub>T</sub></i> (%)	Thickness reduce per rolling <i>r<sub>i</sub></i> (%)	Length Al (mm)	Length increase Al (%)	Length Cu (mm)	Length increase Cu (%)	Width Al wAl (mm)	Width increase Al (%)	Width Cu wCu (mm)	Width increase Cu (%)	Force per rolling <i>FR</i> (Nt)	Torque per rolling <i>TR</i> (Nm)
0	8.8	0	0	53.3	0	53.3	0	13.7	0	13.7	0	0	0
1	8.6	2.27	2.27	54.8	2.81	54.8	2.81	13.88	1.31	13.8	0.73	13577	167.5
2	8.11	7.84	5.70	58	8.82	-	-	15.06	9.93	13.8	0.73	23946	243.69
3	7.64	13.18	5.80	60.12	12.80	-	-	16.8	22.63	13.8	0.73	28671	607.52
4	7.19	18.30	5.89	63.04	18.27	-	-	18.36	34.01	13.88	1.31	30479	285.57
5	6.66	24.32	7.37	67.03	25.76	-	-	19.41	41.68	14.14	3.21	-	-
6	6.08	30.91	8.71	71.8	34.71	-	-	20.19	47.37	14.24	3.94	35584	463.76
7	5.45	38.07	10.36	78.01	46.36	65.26	22.44	20.86	52.26	14.37	4.89	37744	818.17
8	5.04	42.73	7.52	82.83	55.40	68.41	28.35	21.1	54.01	14.44	5.40	34425	449.05
9	4.56	48.18	9.52	90.96	70.66	74.45	39.68	21.45	56.57	14.52	5.99	35747	673.62
10	3.94	55.23	13.60	101.88	91.14	83.06	55.83	21.72	58.54	14.57	6.35	41985	916.53
11	3.12	64.55	20.81	121.16	127.32	100.79	89.10	22.08	61.17	15.62	14.01	54659	1281.34

**Table 4:** Parameters of cold rolling for specimen B

Rolling pass number <i>i</i>	Total thickness <i>h<sub>T</sub></i> (mm)	Total thickness reduce <i>r<sub>T</sub></i> (%)	Thickness reduce per rolling <i>r<sub>i</sub></i> (%)	Length Al (mm)	Length increase Al (%)	Length Cu (mm)	Length increase Cu (%)	Width Al <i>w<sub>Al</sub></i> (mm)	Width increase Al (%)	Width Cu <i>w<sub>Cu</sub></i> (mm)	Width increase Cu (%)	Force per rolling <i>FR</i> (Nt)	Torque per rolling <i>TR</i> (Nm)
0	8.75	0	0	53.25	0	53.25	0	13.6	0	13.8	0	0	0
1	7.82	10.63	10.63	58.21	9.31	54.29	1.95	15.6	14.71	13.8	0.00	32655	324.5
2	6.81	22.17	12.92	63.95	20.09	57.2	7.42	18.03	32.57	13.9	0.72	39760	593.89
3	5.95	32.00	12.63	69.95	31.36	61.17	14.87	19.5	43.38	14.11	2.25	38224	656.06
4	5.04	42.40	15.29	76.92	44.45	68.09	27.87	20.61	51.54	14.42	4.49	45179	859.65
5	3.92	55.20	22.22	94.01	76.54	83.4	56.62	21.47	57.87	15.09	9.35	52081	1307.62
6	3.06	65.03	21.94	114.43	114.89	101.48	90.57	21.9	61.03	15.58	12.90	54822	1328.11

**Table 5:** Variation of the specimens' dimensions due to cold rolling

Specimen	Number of rolling passes	Total thickness reduce <i>r<sub>T</sub></i> (%)	Al thickness reduce <i>r<sub>Al</sub></i> (%)	Cu thickness reduce <i>r<sub>Cu</sub></i> (%)	Al width increase <i>w<sub>Al</sub></i> (%)	Cu width increase <i>w<sub>Cu</sub></i> (%)	Al length increase (%)	Cu length increase (%)
A	11	64.5	73.3	58.5	61.2	14.0	127.3	89.1
B	6	65.0	74.5	56.5	61.0	12.9	114.9	90.6

**Table 6:** Vickers hardness before and after cold rolling for both specimens

Specimen	Al HV hardness			Cu HV hardness		
	Before cold rolling	After cold rolling	Variation	Before cold rolling	After cold rolling	Variation
A	55	67	21,82%	134	167	24,63%
B	55	63	14,55%	134	155	15,67%

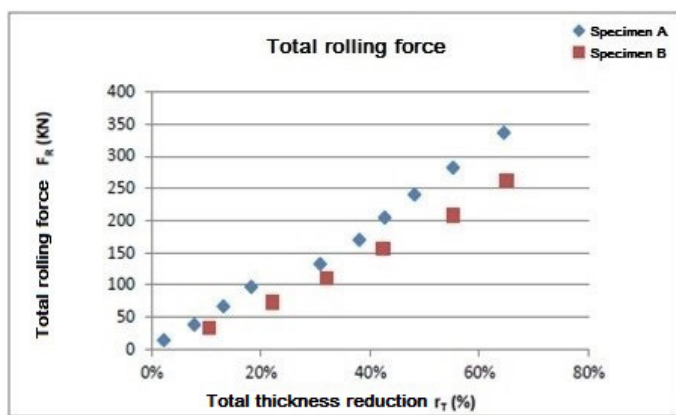


**Figure 3:** Variation of total rolling force with total thickness reduction for specimens A and B

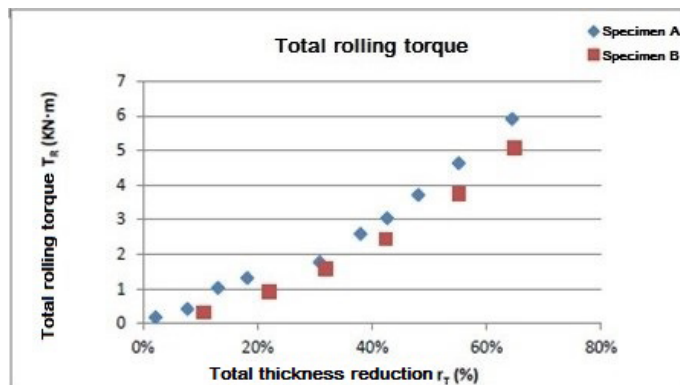


**Figure 4:** Variation of total rolling torque with total thickness reduction for specimens A and B

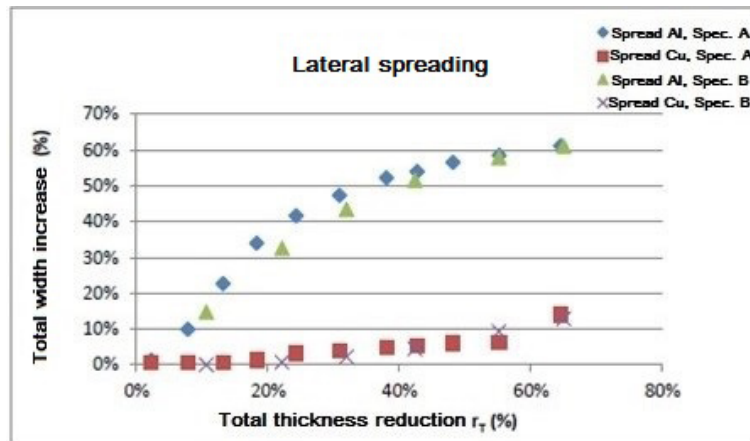


Figure 5: Variation of total width increase (spread) with /total thickness reduction for all layers of specimens A and B

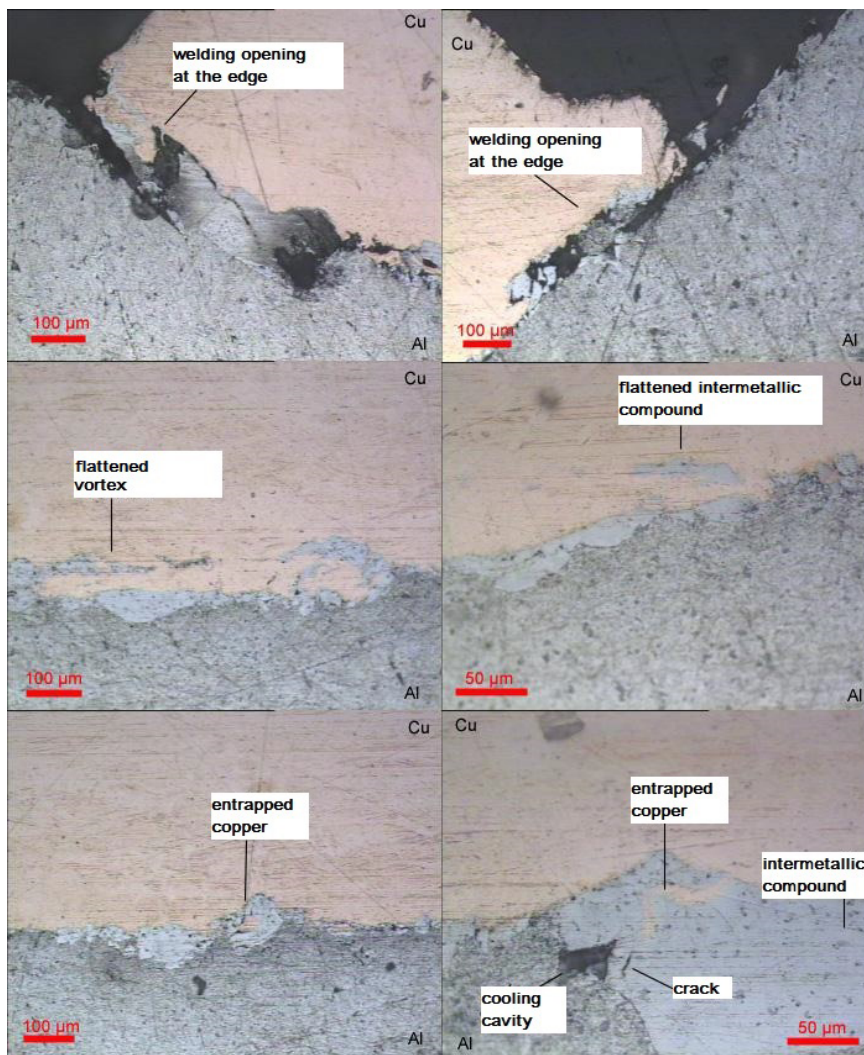


Figure 6: Microstructural characteristics of the aluminum-copper welding interface of specimen A after cold rolling; microscope lens X20, X50

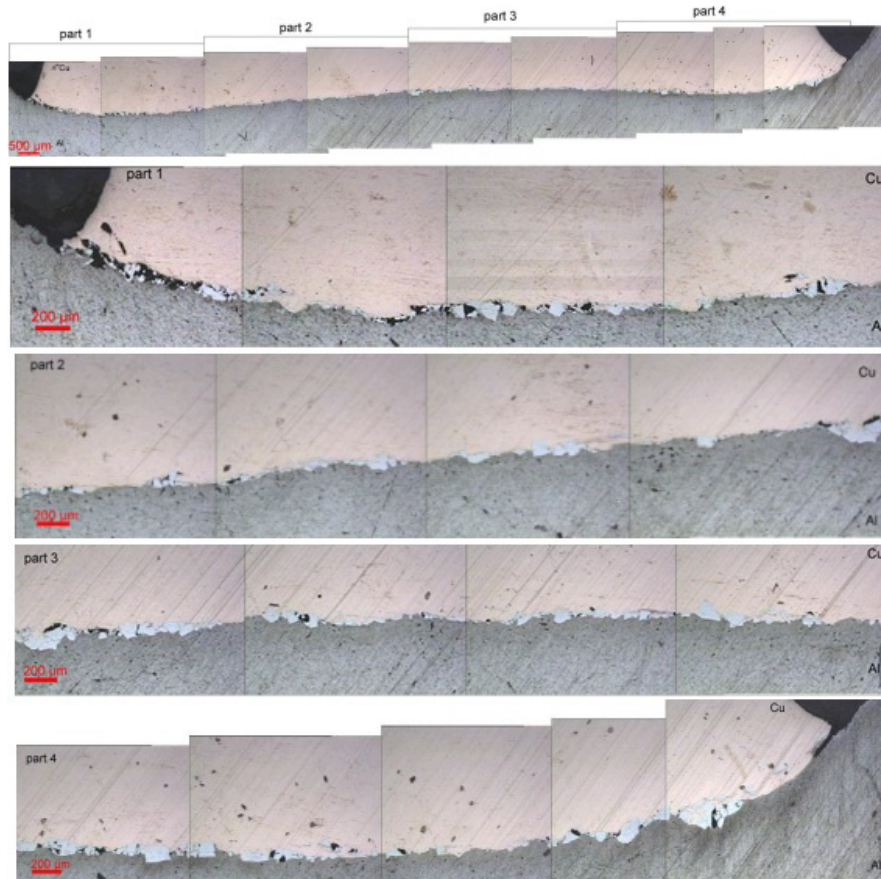


Figure 7: Aluminum-copper welding interface of specimen A after cold rolling; microscope lens X10

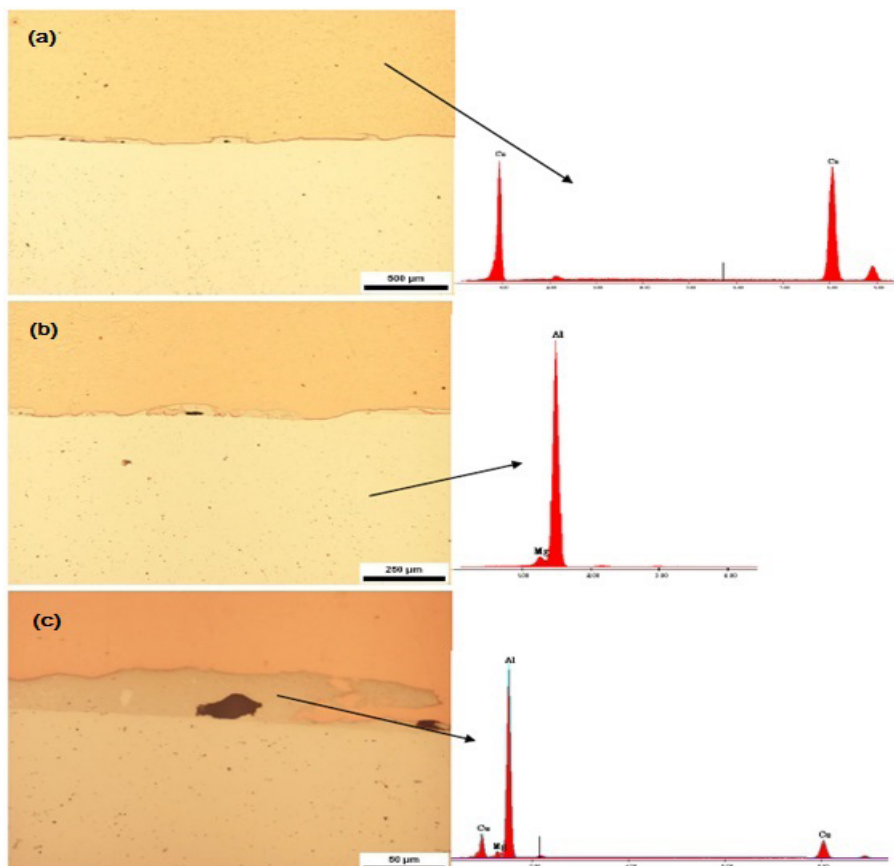


Figure 8: Scanning electron micrographs of the aluminum-copper welding interface and elemental microanalysis spectrum EDS of: (a) Cu, (b) Al and (c) intermetallic compound, specimen A before cold rolling

**Table 7:** Chemical composition of the intermetallic compound (specimen A)

Layer	Element	wt %	at %
Al	Al	95.5	95
	Mg	4.5	5
Intermetallic compound	Mg	3.8	4.7
	Al	80.1	87.7
	Cu	16.1	7.4

secondary tensile stresses developed during the rolling processes were quite high, resulting in limited failure modes, such as lateral spread and folding material at the edge of the specimens. Rolling pass thicknesses of 0.5 mm and 1 mm, for specimens A and B respectively, were selected to limit the intensely deforming phenomena characterizing cold rolling operations with large thickness reduction.

As it can be seen in Figure 3, each point of the total rolling force versus total thickness reduction diagram corresponds to the rolling force value of the current rolling pass increased by the total rolling force of the previous passes. Therefore, the vertical distance between two points corresponds to the rolling force per pass.

From Figures 3 and 4 it be concluded that both rolling force and torque increase with increasing total thickness reduction in a slightly parabolic manner. For specimen A, which experienced about twice as many rolling passes from specimen B, the gradient of both curves is slightly greater. This is a result of the combined effect of work-hardening, which increases by increasing the number of passes, and plastic deformation on specimens'

surfaces. However, a complete work-hardening phenomenon is not particularly evident, since there is no constant value for both force and torque in the final part of the curves.

In Figure 5 the lateral spreading behavior of both specimens is presented. It is evident that lateral spreading increases with increasing total thickness reduction. The final lateral spread value of the aluminum layer is the same for both specimens, a behavior that can also be observed for the copper layer. More specifically, the width increase for the aluminum layer reached the 61 % for both specimens A and B. The corresponding copper layer's width increase was 14 % for specimen A and 12.9 % for specimen B. These different values of lateral spread between the two layers of each bimetallic specimen are due to the aluminum's low Young's Modulus in comparison with copper. The lateral spreading behavior of the copper layer does not appear to be changing depending on the number of passes. However, although the first and last values of the aluminum layer are equal for specimens A and B, intermediate values vary considerably. By increasing the number of rolling passes, aluminum layer's behavior results into a steeper curve, i.e., for the same thickness reduction, an

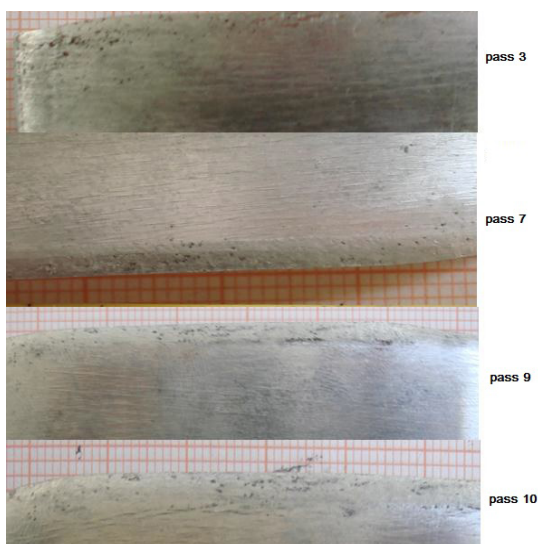


**Figure 9:** Aluminum surface defects of specimen A in different passes

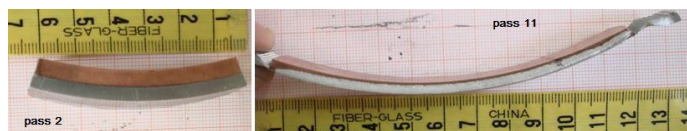


**Figure 10:** Curvature of specimen A after 2 and 11 passes

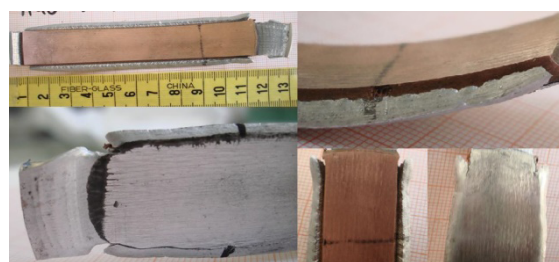


**Figure 11:** Cracks and disruption at the edge of specimen A, after 11 passes



**Figure 12:** Specimens A and B after the cold rolling process

increased lateral spread corresponds to the rolling operation with more passes. Both specimens' initial width/thickness ratio was very low and, consequently, their lateral spread was quite considerable. On the lateral spread areas, surface defects in the aluminum layer were observed, see Figure 9. These defects seem to worsen for each new pass of the rolling operation; see similar observations in Ref. [10].

The elongation occurred from the rolling process was different for each layer of the specimens, see Tables 3 and 4. Specimen's A aluminum layer's length increase was 127.32 % and copper layer's 89.10 %. Specimen's B respective values were 114.89 % and 90.57%. These extension differences led to a curvature of the bimetallic specimen, as can be seen in Figure 10. As a result of this curvature, compressive stresses were developed at the center of the specimens and tensile stresses at their front and back edges, in the rolling direction. Due to these stresses, cracks and disruption were observed at the edges of specimen A, together with excess material at the front edge and folding material at the back edge, see Figure 11. From Figure 12 it is evident that specimen B had the same lateral spreading behavior, cracks, disruption, and surface defects as specimen A.

#### **Effect of the cold rolling process on the bimetallic specimen's hardness**

Vickers hardness measurements performed, before and after cold rolling, on the prepared for metallographic investigation specimens. Hardness values for each specimen are presented in Table 6. It is evident that the rolling process increased the hardness value of both specimens. The rolling process causes creation of dislocations and disorders of the crystal lattice, both of which lead to increase of the yield point and decrease of the ductility of the bimetallic specimen's layers.

The combined effect of the plastic deformation along the whole thickness of the specimen and the work-hardening resulted in higher hardness values for the rolling sequence with more passes of lower thickness reduction (specimen A), in comparison with the rolling sequence with less passes of higher thickness reduction (specimen B). For both specimens the maximum hardness increase after cold rolling achieved on the copper layer. Thus, the hardness increase for the copper layer of specimen A, which underwent 11 passes of cold rolling, was 24.63 % and for the respective copper layer of specimen B, which underwent 6 passes of cold rolling, was 15.67 %; see Table 6. Similar results were obtained for the aluminum layers whose respective values were 21.82 % and 14.55 %.

#### **Microstructural characterization**

The main microstructural features of the Al/Cu interface of the explosively welded bimetallic specimen A after cold rolling, i.e., crack, cooling cavity and intermetallic compound, are presented in Figure 6. Since the microstructure, the elemental microanalysis spectrum and the defects of both specimens were exactly the same, only results pertaining to specimen A are presented.

Microstructure of the Al/Cu-interface in the transverse section, along the explosive welding and rolling direction, together with detailed views of the whole interface can be seen in Figure 7. Figure 8 presents scanning electron micrographs and elemental microanalysis spectrum of the interface before cold rolling.

Along the welding direction a brittle discontinuous intermetallic layer can be detected in Figure 7 – detailed views. The thickness of this layer increased locally in the small transition zone at the center of the specimen. At the back edge of the specimen (left edge), where folding material was developed, many welding openings can be detected, resulting in a non-proper bonding. Therefore, it may be concluded that at this edge the rolling operation destroyed the explosive welding bonding of the metallic components of the specimen. However, at the front edge, where excess material was detected, only a small welding opening may be observed, the size of which is not possible to affect the integrity of the explosive welding interface bonding.

It is evident that the average size of the discontinuous intermetallic regions is bigger from the front edge to the center of the specimen and considerably smaller in the region starting just after the center until the back edge of the specimen. From this observation may be concluded that, along with the excess material, a stress accumulation mechanism occurs at the front end of the specimen leading to a stronger fracture effect on the previously continuous intermetallic layer. After the rolling of the center of the specimen a stress relieving mechanism takes place leading to a more uniform fracture mode. This conclusion is supported by the small cracks detected close to the nearby broken intermetallic regions cavities of the front half specimen. These cracks tend to disappear on the back half specimen or still exist in a considerably smaller size.

As it is evident from Figure 9, the morphology of the explosive welding interface remains wavy even after a multiple-pass cold rolling operation. After explosive welding, intermetallic compounds of the interface can be mostly observed in a vortex form [10,28]. Many of these previous vortices, after the rolling operation, broke and turned into flattened intermetallic compounds, see Figure 6. The biggest of these vortices deformed more than the smaller during the rolling operation creating a considerable amount of new entrapped copper regions.

#### **Conclusions**

Explosively welded bimetallic Al/Cu specimens underwent two different cold rolling processes, which included different number of passes and different thickness reduce per pass, in order to investigate their formability and to determine if a cold rolling process is able to improve their properties. Through the experimental study performed the following general conclusions may be drawn:

Both rolling force and torque increase with increasing total thickness reduction in a slightly parabolic manner, see Figures 3 and 4. For the specimen which underwent twice as many rolling

passes in comparison with the other specimen, the gradient of both curves is slightly greater as a result of the combined effect of work-hardening and plastic deformation on specimens' surfaces. However, a complete work-hardening phenomenon is not particularly evident.

The lateral spreading of the specimens increases with increasing total thickness reduction. The final lateral spread value of the aluminum layer is the same for both specimens and it is considerably greater than the lateral spread of the copper layer, which is also the same for both specimens, see Figure 5. On the lateral spread areas, surface defects of the aluminum layer were observed, which seem to worsen for each new pass of the rolling operation, as can be seen in Figure 9.

Due to the compressive stresses developed at the center of the specimens and the tensile stresses at their front and back edges, as a result of the different extension of each layer which led to a curvature, cracks and disruption were observed at the edges of the specimens, together with excess material at the front edges and folding material at the back edges, see Figure 11.

Hardness values were higher for the specimen which underwent a rolling process with more passes of lower thickness reduction, in comparison with the specimen which underwent a rolling process with less passes of higher thickness reduction. For both specimens the maximum hardness increase after cold rolling achieved on the copper layer.

At the back edge of the specimens, where folding material was developed, many welding openings can be detected, resulting in a non-proper bonding. Therefore, it may be concluded that at this edge the rolling operation destroyed the explosive welding bonding of the two layers of the specimens. However, at the front edge, where excess material was detected, only a small welding opening may be observed in both specimens, the size of which is not possible to affect the integrity of the explosive welding interface bonding.

Along with the excess material, a stress accumulation mechanism occurs at the front end of the specimens leading to a stronger fracture effect on the previously continuous intermetallic layer. After the rolling of the center of the specimen a stress relieving mechanism takes place leading to a more uniform fracture mode. This conclusion can also be supported by the observation of small cracks close to the nearby broken intermetallic regions cavities of the front half specimen which tend to disappear on the back half specimen or still exist in a considerably smaller size.

After explosive welding, intermetallic compounds of the interface can be mostly observed in a vortex form [29], many of which, after the rolling operation, broke and turned into flattened intermetallic compounds, see Figure 6. The biggest of these vortices deformed more than the smaller during the rolling operation creating a considerable amount of new entrapped copper regions.

As an overall conclusion it can be noted that even though cold rolling improves the hardness of both layers of explosively welded bimetallic Al/Cu specimens, yet it is not a suitable post welding process for this type of specimens since it affects detrimentally the structure of the intermetallic bonding layer obtained by the explosive welding operation and consequently weaken it.

## References

1. Lysak VI, Kuzmin SV. Energy balance during explosive welding. *Journal of Materials Processing Technology*. 2015; 222:356–364. doi: <https://doi.org/10.1016/j.jmatprotec.2015.03.024>.
2. Mendes R, Ribeiro JB, Loureiro A. Effect of explosive characteristics on the explosive welding of stainless steel to carbon steel in cylindrical configuration. *Materials and Design*. 2013; 51:182-192. doi: <https://doi.org/10.1016/j.matdes.2013.03.069>.
3. Rajani HZ, Mousavi SA. The effect of explosive welding parameters on metallurgical and mechanical interfacial features of Inconel 625/plain carbon steel bimetal plate. *Materials Science & Engineering A*. 2012; 556:454-464. doi: <https://doi.org/10.1016/j.msea.2012.07.012>.
4. Wang Y, Beom HG, Sun M, Lin S. Numerical simulation of explosive welding using the material point method. *International Journal of Impact Engineering*. 2011; 38(1):51-60. doi: <https://doi.org/10.1016/j.ijimpeng.2010.08.003>.
5. Wang X, Zheng Y, Liu H, Shen Z, Hu Y, Li W, et al. Numerical study of the mechanism of explosive/impact welding using Smoothed Particle Hydrodynamics method. *Materials and Design*. 2012; 35:210-219. doi: <https://doi.org/10.1016/j.matdes.2011.09.047>.
6. Mousavi AA, Al-Hassani STS. Numerical and experimental studies of the mechanism of the wavy interface formations in explosive/impact welding. *Journal of the Mechanics and Physics of Solids*. 2005; 53(11):2501–2528. doi: <https://doi.org/10.1016/j.jmps.2005.06.001>.
7. Athar MH, Tolaminejad B. Weldability window and the effect of interface morphology on the properties of Al/Cu/Al laminated composites fabricated by explosive welding. *Materials and Design*. 2015; 86:516–525. doi: <https://doi.org/10.1016/j.matdes.2015.07.114>.
8. Akbari-Mousavi SAA, Barrett LM, Al-Hassani STS. Explosive welding of metal plates. *Journal of Materials Processing Technology*. 2008; 202(1-3):224–239. doi: <https://doi.org/10.1016/j.jmatprotec.2007.09.028>.
9. Wypart J, Rydz D, Stradomski G, Dyja H. Analysis of bimetallic plate rolling after explosive welding. *Archives of Metallurgy and Materials*. 2014; 59(4):1571-1573.
10. Mamalis AG, Vaxevanidis NM, Szalay A, Prohaszka J. Fabrication of aluminium/copper bimetals by explosive cladding and rolling. *Journal of Materials Processing Technology*. 1994; 44:99-117.
11. Crossland B. *Explosive Welding of Metals and Its Application*. Oxford Series of Advanced Manufacturing, Oxford, UK; 1982.
12. Blazynski TZ, editor. *Explosive welding, forming and compaction*. Germany: Springer; 2012.
13. Grignon F, Benson D, Vecchio KS, Meyers MA. Explosive welding of aluminum to aluminum: analysis, computations and experiments. *International Journal of Impact Engineering*. 2004; 30(10):1333-1351.

14. Dyja H, Mróz S, Milenin A. Theoretical and experimental analysis of the rolling process of bimetallic rods Cu-steel and Cu–Al. *Journal of Materials Processing Technology*. 2004; 153:100-107.
15. Chen H, Yang L, Long J. First-principles investigation of the elastic, Vickers hardness and thermodynamic properties of Al–Cu intermetallic compounds. *Superlattices and Microstructures*. 2015; 79:156-165. doi: <https://doi.org/10.1016/j.spmi.2014.11.005>.
16. Lassnig A, Pelzer R, Gammer C, Khatibi G. Role of intermetallics on the mechanical fatigue behavior of Cu-Al ball bond interfaces. *Journal of Alloys and Compounds*. 2015; 646:803-809. doi: <https://doi.org/10.1016/j.jallcom.2015.05.282>.
17. Bataev IA, Bataev AA, Mali VI, Pavliukova DV. Structural and mechanical properties of metallic–intermetallic laminate composites produced by explosive welding and annealing. *Materials and Design*. 2012; 35:225-234. doi: <https://doi.org/10.1016/j.matdes.2011.09.030>.
18. Zhang LJ, Pei Q, Zhang JX, Bi ZY, Li PC. Study on the microstructure and mechanical properties of explosive welded 2205/X65 bimetallic sheet. *Materials and Design*. 2014; 64:462-476. doi: <https://doi.org/10.1016/j.matdes.2014.08.013>.
19. Kahraman N, Gülenç B, Findik F. Joining of titanium/stainless steel by explosive welding and effect on interface. *Journal of Materials Processing Technology*. 2005; 169(2):127-133. doi: <https://doi.org/10.1016/j.jmatprotec.2005.06.045>.
20. Zhang N, Wang W, Cao X, Wu J. The effect of annealing on the interface microstructure and mechanical characteristics of AZ31B/AA6061 composite plates fabricated by explosive welding. *Materials and Design*. 2015; 65:1100-1109. doi: <https://doi.org/10.1016/j.matdes.2014.08.025>.
21. Xie MX, Zhang LJ, Zhang GF, Zhang JX, Bi ZY, Li PC. Microstructure and mechanical properties of CP-Ti/X65 bimetallic sheets fabricated by explosive welding and hot rolling. *Materials and Design*. 2015; 87:181-197. doi: <https://doi.org/10.1016/j.matdes.2015.08.021>.
22. Durgutlu A, Gülenç B, Findik F. Examination of copper/stainless steel joints formed by explosive welding. *Materials and Design*. 2005; 26(6):497-507. doi: <https://doi.org/10.1016/j.matdes.2004.07.021>.
23. Song JL, Lin SB, Yang CL, Fan CL. Effects of Si additions on intermetallic compound layer of aluminum-steel TIG welding-brazing joint. *Journal of Alloys and Compounds*. 2009; 488:217-222.
24. Cowan GR, Bergmann OR, Holtzman AH. Mechanism of bond zone wave formation in explosion-clad metals. *Metallurgical and Materials Transactions B*. 1971; 2(11):3145-3155.
25. Jaramillo D, Szecket A, Inal OT. On the transition from a waveless to a wavy interface in explosive welding. *Materials Science and Engineering*. 1987; 91:217-222.
26. Bazdenkov SV, Demichev VF, Morozov DK, Pogutse OP. Possible mechanism of wave formation in explosive welding, *Combustion, Explosion and Shock Waves*. 1985; 21(1):124-130.
27. Asemabadi M, Sedighi M, Honarpisheh M. Investigation of cold rolling influence on the mechanical properties of explosive-welded Al/Cu bimetal. *Materials Science & Engineering A*. 2012; 558:144-149.
28. Bataev AI, Bataev AA, Mali VI, Bataev VA, Balaganskii IA. Structural changes of surface layers of steel plates in the process of explosive welding. *Met. Sci. Heat Treat*. 2014; 55(9-10):509-513. doi: [10.1007/s11041-014-9663-7](https://doi.org/10.1007/s11041-014-9663-7).